Program Digest, 2019 IEEE International Ultrasonics Symposium (IUS)
Glasgow, Scotland, October 6-9, 2019

Nondestructive evaluation of residual stress through acoustically stimulated electromagnetic response in welded steel

Yuhei Suzuki
Department of Applied Physics
Tokyo University of A & T
Tokyo, Japan
IHI Inspection & Instrumentation Co., Ltd.
Yokohama, Japan
s175294y@st.go.tuat.ac.jp

Yuichi Ichikawa
Department of Applied Physics
Tokyo University of A & T
Tokyo, Japan
you1.ichikawa@gmail.com

Hisato Yamada
Department of Applied Physics
Tokyo University of A & T
Tokyo, Japan
h-yamada@cc.tuat.ac.jp

Kenji Ikushima
Department of Applied Physics
Tokyo University of A & T
Tokyo, Japan
ikushima@cc.tuat.ac.jp

***Abstract*—Tensile residual stresses combined with an applied tensile stress can reduce the reliability of steel components. Nondestructive evaluation of residual stress is thus important to avoid unintended fatigue or cracking. Because magnetic hysteresis properties of ferromagnetic materials are sensitive to stress, nondestructive evaluation of residual stress through magnetic properties can be expected. The spatial mapping of local magnetic hysteresis properties becomes possible by using the acoustically stimulated electromagnetic (ASEM) method and the tensile stress dependence of the hysteresis properties has been investigated in steel. It is found that the coercivity H_c and the remanent magnetization signal V_r monotonically decrease with increasing the tensile stress. In this work, we verified the detection of residual stresses through the ASEM response in a welded steel plate. Tensile stresses are intentionally introduced on the opposite side of the partially welded face by controlling welding temperatures. We found that H_c and V_r clearly decrease in the welded region, suggesting that the presence of tensile residual stresses is well detected by the hysteresis parameters.**

Keywords—ultrasonic, electromagnetic response, residual stress, steel, nondestructive evaluation

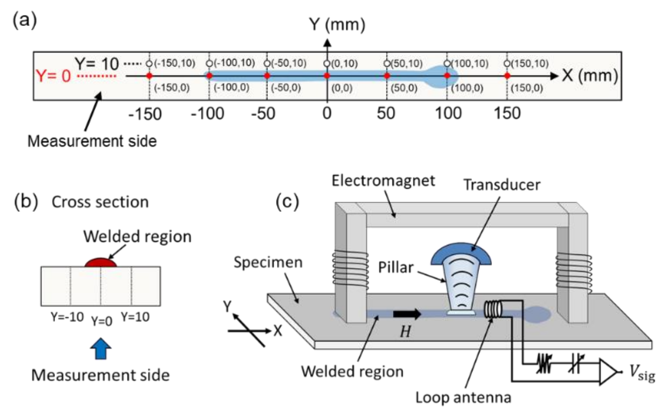

Fig. 1. (a) Coordinates of the opposite side of the partially welded face (measurement side) in a steel plate. The blue region indicates the area discolored by welding in which tensile residual stresses are introduced. (b) Cross sectional view of the welded steel plate. (c) Schematic of ASEM measurement setup.

I. Introduction

Residual stress is an important factor in terms of life time and failure of steel products. Residual stress occurs during fabrication process such as welding, which may greatly impair the strength of steel components. When an applied stress is combined with initial residual stresses, the concentration of tensile stresses often damages engineering components [1], [2]. To avoid the risk of damage, it is important to evaluate the residual stress in actual objects. This information allows to optimize design, fabrication and welding process. Although several stress inspection techniques have been reported [3]-[7], quantitative nondestructive evaluation of residual stress and its spatial mapping are still under development.

Magnetic hysteresis curve contains a number of independent parameters of ferromagnetic materials (coercivity H_c, saturation magnetization or permeability). These hysteresis parameters are sensitive to stress produced in the materials [8], [9]. Consequently, the hysteresis measurements are expected to evaluate residual stress in steel materials. However, the use of magnetic properties for stress evaluation has been limited because conventional hysteresis measurements through electromagnetic induction obtain the bulk properties averaged over the entire sample. Namely, the local hysteresis properties are not probed. However, the spatial mapping of local magnetic hysteresis properties has become possible by ultrasonic focusing and scanning [10]-[13]. This technique is based on the generation and detection of the acoustically stimulated electromagnetic (ASEM) response through the magnetomechanical coupling. Recently, the tensile stress dependence of the hysteresis properties has been investigated by using the ASEM method. It is found that the coercivity H_c and

JSPS KAKENHI Grant Number JP17H02808

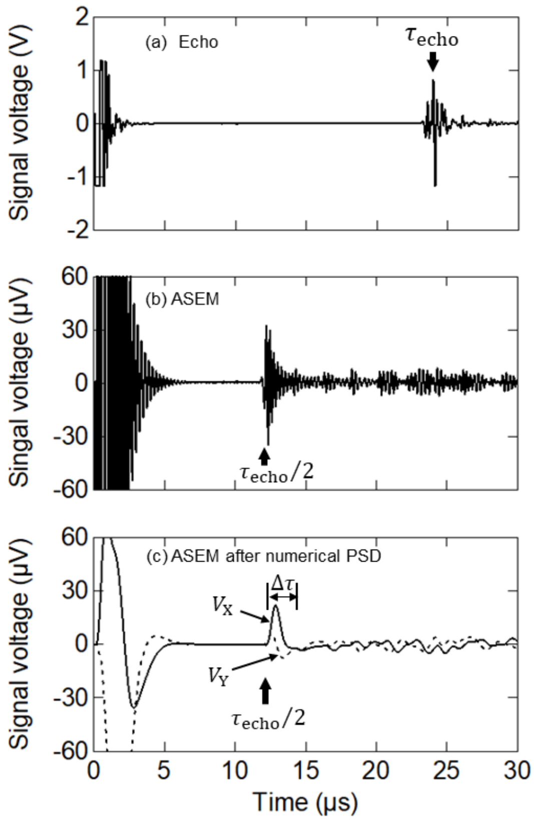

Fig. 2. (a) Real-time echo waveform. (b) Real-time ASEM waveform. (c) The in-phase component, V_X (solid line), and the quadrature component, V_Y (dotted line), after numerical PSD.

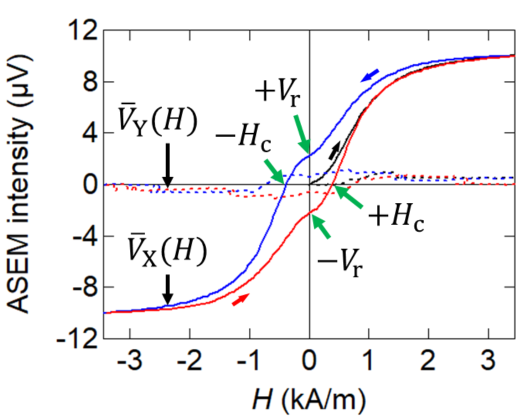

Fig. 3. ASEM hysteresis curves of the welded specimen. The in-phase component, $\bar{V}_X(H)$ (solid line), and the quadrature component, $\bar{V}_Y(H)$ (dotted line). The black, blue, and red lines represent the initial magnetization curve, the downward-field curve, and the upward-field curve, respectively.

the remanent magnetization signal V_r monotonically decrease with increasing the tensile stress [14].

In this work, we verified the detection of residual stresses through ASEM response in a welded steel plate. Tensile stresses

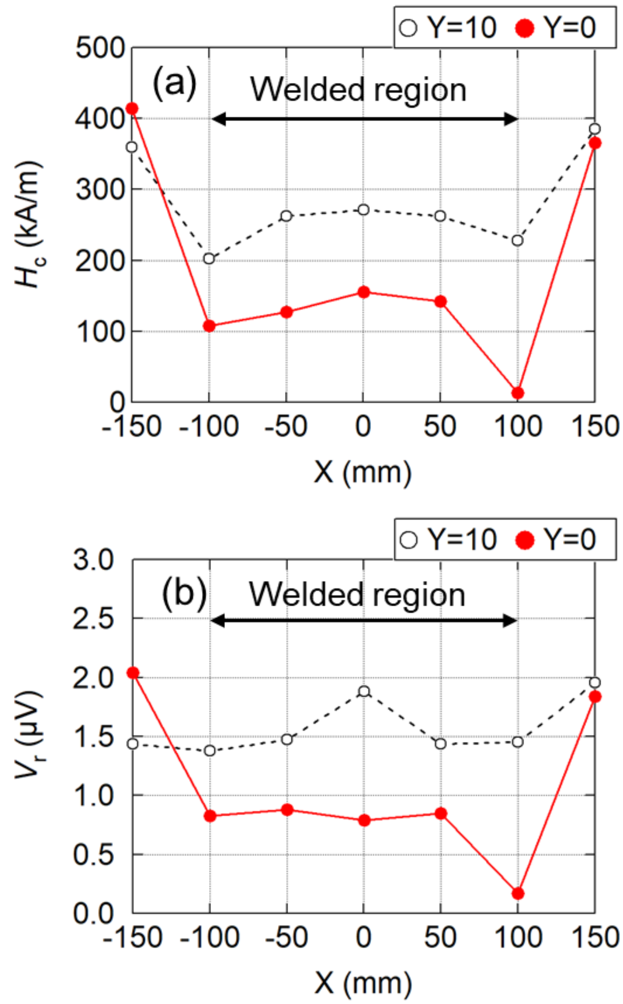

Fig. 4. Spatial distribution of (a) coercivity H_c and (b) remanent magnetization signal V_r along the X axis on the back side of the welded steel plate.

are intentionally introduced on the back side of the welded parts by controlling the welding temperatures. Reduction of the H_c and V_r was observed on the back side of the welded parts.

II. Method

A steel specimen (size : 490 mm × 70 mm × 6 mm) was prepared from a 25-mm-thick carbon steel plate (S25C, JIS G4051:2009) by a machining process (Fig 1(a)). As seen in Figs. 1(a) and 1(b), one face of the steel plate is partially welded by controlling the temperatures so that it does not exceed 550 ℃ on the other face to avoid the phase transformation of crystals. In this heating processes, tensile stresses are introduced on the opposite side of the welded region in the steel plate (the blue region in Fig. 1(a)). The magnetic hysteresis properties were measured on the opposite side of the welded face by using the ASEM method. The ASEM measurements were carried out by using a 4 MHz transducer with an acoustic delay line (polystyrene pillar) (Fig. 1(c)). The signal was picked up through a resonant loop antenna tuned to the ultrasound frequency. Magnetic fields H were applied along the longitudinal direction of the steel plate by using an electromagnet.

Figure 2 represents typical real-time waveforms of echo and ASEM signals. The echo signal from the surface of the specimen was observed at τ_{echo} = 24 μs (Fig. 2(a)). The direct rf signal, $V_{\mathrm{sig}}(t)$, of the ASEM response was observed at half of the echo delay time (τ_{echo}/2 = 12 μs) (Fig. 2(b)). Using a phase-sensitive detection (PSD) scheme, we numerically converted $V_{\mathrm{sig}}(t)$ to the in-phase $V_{\mathrm{X}}(t)$ and quadrature $V_{\mathrm{Y}}(t)$ components (Fig. 2(c)).

In the ASEM hysteresis measurements, the signal voltages $V_{\mathrm{X}}(t)$ and $V_{\mathrm{Y}}(t)$ were plotted as the time-averaged intensities, $\overline{V_{\mathrm{X}}}$ and $\overline{V_{\mathrm{Y}}}$, respectively [13]. Before starting the ASEM measurement, the specimen was demagnetized by applying an alternating current using the electromagnet.

III. Results and Discussion

Figures 3 shows the ASEM hysteresis curves of $\bar{V}_{\mathrm{X}}(H)$ and $\bar{V}_{\mathrm{Y}}(H)$. Because the quadrature component, $\bar{V}_{\mathrm{Y}}(H)$, is negligible in the specimen, we focus on hysteresis parameters obtained from the in-phase component $\bar{V}_{\mathrm{X}}(H)$. We determined the coercivity, H_{c}, and the remanent magnetization signal, V_{r}, as the intercepts of the transversal and longitudinal axes in the $\bar{V}_{\mathrm{X}}(H)$ hysteresis loop, respectively.

Figure 4(a) and 4(b) represent the spatial distribution of H_{c} and V_{r} along the X axis on the opposite side of the welded face, respectively. The results measured along the X axis at $Y = +10$ mm are plotted as reference data at positions shifted from the welded region. We found that the hysteresis parameters H_{c} and V_{r} are reduced directly under the welded region, indicating that the intentionally introduced tensile stresses are well detected. Using the conversion coefficients from hysteresis parameters to tensile stress[14], the residual stress at $(X, Y) = (0, 0)$ is roughly estimated to be about 300 MPa. In this specimen, excess heat is applied at the welding start point $(X, Y) = (+100, 0)$. The minimum observed at $(X, Y) = (+100, 0)$ suggests that plastic deformation occurs due to the excess heat.

IV. Conclusion

To verify the detection of residual stresses, we prepared a welded steel plate in which tensile residual stresses are intentionally introduced on the opposite side of the welded face. We measured the spatial distribution of ASEM hysteresis curves on the opposite side of the welded face. The hysteresis parameters H_{c} and V_{r} were distinctly reduced in the welded region. This feature is reasonably explained by the tensile stress dependence of H_{c} and V_{r} measured by tensile testing.

Acknowledgment

We thank T. Uchida from Nippon Pneumatic Mfg. Co., Ltd. (NPK) for preparing the samples. We also thank T. Ozaki from Denshijiki Industry Co., Ltd. for technical help. This work is financially supported by JSPS KAKENHI Grant Number JP17H02808.

References

[1] P. J. Withers and H. K. D. H. Bhadeshia, “Residual stress. Part 1 - Measurement techniques,” *Mater. Sci. Technol.*, vol. 17, no. 4, pp. 355–365, Apr. 2001.

[2] G.S. Schajer and C. O. Ruud, “Overview of residual stresses and their measurement,” in *Practical Residual Stress Measurement Methods*, Chichester, UK, John Wiley & Sons, 2013, pp. 1-27.

[3] T. Leon-Salamanca and D. F. Bray, “Residual stress measurement in steel plates and welds using critically refracted longitudinal (L_{CR}) waves,” *Res. Nondestruct. Eval.*, vol. 7, no. 4, pp. 169–184, Dec. 1996.

[4] A. Mitra, L. B. Sipahi, M. R. Govindaraju, D. C. Jiles, and V. R. V. Ramanan, “Effects of tensile stress on magnetic Barkhausen emissions in amorphous Fe-Si-B alloy,” *J. Magn. Magn. Mater.*, vol. 153, no. 1-2, pp. 231–234, Feb. 1996.

[5] *Residual Stress Measurement by X-ray Diffraction. SAE J784, Society of Automotive Engineers Handbook Supplement*, SAE International, Warrendale, PA, USA, 2003.

[6] N. Tebedge, G. Alpsten, and L. Tall, “Residual-stress measurement by the sectioning method,” *Exp. Mech.*, vol. 13, no. 2, pp. 88–96, Feb. 1973.

[7] B. Zuccarello, “Optimal calculation steps for the evaluation of residual stress by the incremental hole-drilling method”, *Exp. Mech.*, vol. 39, no. 2, pp. 117–124, Jun. 1999.

[8] D. Jiles, *Introduction to Magnetism and Magnetic Materials*, 3rd ed., Boca Raton, FL, USA, CRC Press, 2016, p. 421.

[9] J. M. Makar and B. K. Tanner, “The effect of plastic deformation and residual stress on the permeability and magnetostriction of steels,” *J. Magn. Magn. Mater.*, vol. 222, no. 3, pp. 291-304, Dec. 2000.

[10] K. Ikushima, S. Watanuki, and S. Komiyama, “Detection of acoustically induced electromagnetic radiation”, *Appl. Phys. Lett.*, vol. 89, no. 19, pp. 194103(1-3), 2006.

[11] H. Yamada, K. Takashima, K. Ikushima, H. Toida, M. Sato, and Y. Ishizawa, ″Magnetic sensing via ultrasonic excitation,” *Rev. Sci. Instrum.*, vol. 84, no. 4, pp. 044903(1-5), 2013.

[12] H. Yamada, K. Watanabe, and K. Ikushima, ″Magnetic hysteresis and magnetic flux patterns measured by acoustically stimulated electromagnetic response in a steel plate,” *Jpn. J. Appl. Phys.*, vol. 54, no. 8, pp. 086601(1-4), 2015.

[13] H. Yamada, J. Yotsuji, and K. Ikushima, ″Phase-sensitive detection of acoustically stimulated electromagnetic response in steel,” *Jpn. J. Appl. Phys.*, vol. 57, no. 7S1, pp. 07LB09(1-5), 2018.

[14] Y. Suzuki, H. Yamada, T. Ozaki, and K. Ikushima, “Stress dependence of magnetic hysteresis properties through acoustically stimulated electromagnetic response in steel,” in *Proc. IEEE Int. Ultrason. Symp. (IUS)*, Oct. 2018, pp. 1–4.